2023

Synergistic Ti-Fe Oxides on Fishbone-Derived Carbon Sulfonate: Enhanced Styrene Oxidation Catalysis

Mukhamad Nurhadi, *Universitas Mulawarman*
Ratna Kusumawardani, *Universitas Mulawarman*
Teguh Wirawan, *Universitas Mulawarman*
Sin Yuan Lai, *Xiamen University Malaysia*
Hadi Nur, *Universitas Negeri Malang*

Synergistic Ti-Fe Oxides on Fishbone-Derived Carbon Sulfonate: Enhanced Styrene Oxidation Catalysis

Mukhamad Nurhadi[1*], Ratna Kusumawardani[1], Teguh Wirawan[2], Sin Yuan Lai[3,4,5], and Hadi Nur[6,7]

[1]*Department of Chemical Education, Universitas Mulawarman, Kampus Gunung Kelua, Samarinda 75119, Indonesia*

[2]*Department of Chemistry, Faculty of Mathematics and Natural Sciences, Universitas Mulawarman, Samarinda 75119, Indonesia*

[3]*School of Energy and Chemical Engineering, Xiamen University Malaysia, Selangor Darul Ehsan 43900, Malaysia*

[4]*Kelip-kelip! Center of Excellence for Light Enabling Technologies, Xiamen University Malaysia, Bandar Sunsuria, Sepang 43900, Malaysia*

[5]*College of Chemistry and Chemical Engineering, Xiamen University, Xiamen 361005, China*

[6]*Department of Chemistry, Faculty of Mathematics and Natural Sciences, Universitas Negeri Malang, Jl. Semarang No. 5, Malang 65145, Indonesia*

[7]*Center of Advanced Materials for Renewable Energy (CAMRY), Universitas Negeri Malang, Jl. Semarang No. 5, Malang 65145, Indonesia*

* ***Corresponding author:***

email: nurhadi1969@yahoo.co.id

Received: December 27, 2022
Accepted: September 26, 2023

DOI: 10.22146/ijc.80667

Abstract: *Fishbone-derived carbon sulfonate, modified through incipient wetness impregnation with titanium tetraisopropoxide and iron nitrate salts, displays catalytic activity in the oxidation of styrene with hydrogen peroxide (H_2O_2) as an oxidant. This was done to develop a cost-effective, non-toxic, and environmentally friendly bimetallic oxide catalyst, incorporating titanium and iron oxides on mesoporous-derived carbon fishbone to enhance styrene conversion and benzaldehyde selectivity in styrene oxidation using aqueous H_2O_2. The catalyst, featuring a combination of titanium and iron oxides on the surface of the fishbone-derived carbon sulfonate, demonstrates higher catalytic activity than single oxide catalysts, such as titanium or iron oxides alone. Factors influencing the catalyst's performance are investigated by using FTIR, XRD, XRF, SEM, and BET surface area. The results reveal that the presence of both titanium and iron oxides on the surface of the fishbone-derived carbon sulfonate and the catalyst's surface area creates a synergistic effect, the primary factors affecting its catalytic activity in styrene oxidation using H_2O_2 as an oxidant.*

Keywords: *iron; oxidation; styrene; synergistic effect; titanium*

■ INTRODUCTION

The styrene oxidation on various transition metal-substituted catalysts remains a topic of significant interest in both academic and commercial fields. The process is crucial for synthesizing three vital products, namely styrene oxide, phenylacetaldehyde, and benzaldehyde, using hydrogen peroxide (H_2O_2) [1-3]. Benzaldehyde, the primary product of styrene oxidation, is an industrially important and versatile organic compound. It is extensively used as a key intermediate in synthesizing perfume materials, anthelmintics, epoxy resins, plasticizers, drugs, sweeteners, chiral pharmaceuticals, pesticides, and epoxy paints [4-6]. Currently, two processes are employed for industrial production: (1) toluene reacts with oxygen to give benzoic acid in the catalytic oxidation, and (2) the hydrolysis of benzyl chloride [7-8]. It is significant to note that both catalytic oxidation and hydrolysis reactions demonstrate some crucial drawbacks, including high energy consumption, extended reaction duration, and the generation of

chloride waste. These issues have resulted in inferior conversion performance, low benzaldehyde yield (up to 20%) and selectivity. Contrarily, styrene selective oxidation could be a more appealing alternative compared to those complex approaches, drastic conditions, and toxic waste disposal of existing procedures. In an effort to elevate styrene catalytic oxidation, benzaldehyde yield, and selectivity, the utilization of heterogeneous catalysts is generally deemed more promising, particularly those containing transition metals as active sites.

Developing a bimetallic oxide heterogeneous oxidation catalyst, which combines titanium and iron oxides as active sites, while the catalyst support consists of carbon mesoporous-derived fishbone, offering an approach to enhance the catalytic activity. This catalyst system offers advantages, such as being cost-effective, innocuous, and eco-friendly. To further validate the advantages bestowed by this catalytic system design, the bimetallic composite was compared with monometallic transition metals (Ti or Fe), which both were supported onto carbon-derived fish bones. The catalytic activity of these two systems was investigated in a model reaction, namely an oxidation reaction containing styrene with aqueous H_2O_2.

The styrene oxidation using H_2O_2 has been studied using monometallic oxide transition metals supported on different materials as catalysts. This is one of the reactions that can be employed as it is interesting from both industrial and scientific perspectives. Examples of monometallic transition metals introduced onto material support in styrene oxidation reactions include MCM-48 [9], Cu [10], Pd [11], La [6], Ti [7,12-14], Mn [15-16], Fe [13], V [17], and Cr [18]. However, styrene conversion and benzaldehyde selectivity remain low when monometallic transition metals are used on diverse material supports as catalysts.

Recently, numerous researchers have become increasingly interested in examining bimetallic oxides supported on various materials as catalysts. Bimetallic catalysts, composed of two different metals, exhibit unique characteristics. The synergistic effects of bimetallic oxide catalysts often result in novel physicochemical properties that render the catalyst superior to either monometallic oxide component [19]. Bimetallic oxide catalysts have been extensively applied in the oxidation reactions. Several bimetallic catalysts have been explored to augment styrene conversion and benzaldehyde selectivity in styrene oxidation, such as MOF-74(Cu/Co) [3], Mn, Co-MCM-41 [20], La–Zn bimetallic oxide [21], CoNiPW [22], Cux-Coy-MOF [23], and Co–Vanadium oxide supported on reduced graphene [24].

It reveals that despite the advances in bimetallic catalysts, there is still room for improvement in styrene conversion and benzaldehyde selectivity. The proposed novel bimetallic oxide catalyst system, consisting of titanium and iron oxides supported on carbon mesoporous-derived fishbone, has the potential to address these challenges. This innovative approach aims to enhance the catalytic performance while offering the benefits of being cost-effective, non-toxic, and environmentally friendly.

This study systematically investigated the catalytic activity and selectivity of the titanium and iron bimetallic oxide catalyst supported on carbon mesoporous-derived fishbone in the styrene oxidation reaction using aqueous H_2O_2 as an oxidant. We compared the performance of this bimetallic catalyst with those of monometallic transition metal (Ti or Fe) catalysts supported on carbon-derived fish bones. Additionally, we will explore the effect of varying the metal ratio, catalyst loading, and reaction conditions (e.g., temperature, pressure, and reaction time) on the catalytic performance.

By addressing the existing gap in the research, our study aims to develop a more efficient and environmentally friendly catalyst system for styrene oxidation. This would not only contribute to the advancement of knowledge in the field of heterogeneous catalysis but also provide potential industrial applications, particularly in the synthesis of valuable chemicals such as benzaldehyde and its derivatives. Ultimately, the successful development and implementation of this bimetallic oxide catalyst system could significantly improve the efficiency, selectivity, and sustainability of styrene oxidation processes.

■ EXPERIMENTAL SECTION

Materials

Sulfuric acid (H_2SO_4, 97%) was received from JT Beker, Germany. Titanium(IV) isopropoxide ($Ti\{OCH(CH_3)_2\}_4$, 97%) was obtained from Sigma Aldrich, USA. Iron(III) nitrate ($Fe(NO_3)_3$) was ordered from Merck, Germany. Acetone (C_3H_6O, 99.75%) used as solvent was obtained from Mallinckrodt. Ethanol (C_2H_6O, 96%) used as solvent was received from Merck, Germany. Styrene ($C_6H_5CH=CH_2$, 99%) used as the reductant was bought from Sigma Aldrich, USA. Acetonitrile (CH_3CN, 100%) used as solvent was received from Merck, USA. H_2O_2 (30%) used as oxidant was obtained from Merck, USA. Fishbone waste was collected from many companies in Samarinda, Indonesia.

Instrumentation

The equipment and instruments used in this study included a furnace (Thermo Scientific) used for the carbonization process, oven (Memmert), FTIR spectrometer (IR-Prestige-21 Shimadzu), XRD instrument (Phillips PANalytical X'Pert PRO), X-ray fluorescence (WDXRF PANalytical, Minipal 4), SEM (FEI Inspect S50), the nitrogen adsorption-desorption isotherms (Quantachrome NovaWIn instrument version 11.0), GC-2010 Shimadzu-gas chromatography equipped with an SH-Rxi-5ms column (30 m × 0.25 mm ID × 0.25 μm df) (serial 1652111), a flame ionization detector (FID) and nitrogen as the carrier gas.

Procedure

Carbonization process

Carbon was prepared from the fishbone waste from many food companies around Samarinda, East Kalimantan, Indonesia. The fishbone was cleaned from impurities and dried. The fishbone was crushed to powdered form and then carbonized in a furnace at 500 °C for 2 h to form carbon. The fishbone-derived carbon was labeled as FBC.

Sulfonization process

Every 1 g of FBC was soaked in 10 mL of H_2SO_4 (1 M, JT Beker) and stirred at room temperature for 24 h. The mixer was filtered and washed with distillate water to remove any loosely bound acid, and it was dried at 110 °C overnight to obtain sulfonated fishbone-derived carbon (SFBC).

Ti and Fe impregnation

The process of impregnation follows the previous research [12]. Every 1 g of SFBC was impregnated with titanium tetraisopropoxide (500 μmol) and iron(III) nitrate (500 μmol) that was soaked in 10 mL acetone and stirred until all of the acetone solvents completely evaporated. The residual acetone was removed from the SFBC sample with ethanol (Merck) and dried at 110 °C overnight. The amount of Ti and Fe impregnated in the catalysts varied, such as 1:1, 2:1, and 1:2, respectively. Furthermore, the catalysts were calcined at 350 °C for 2 h. The catalysts were denoted as Ti-Fe(x:y)/SFBC, whereas x = concentration of Ti and y = concentration of Fe. For example, Ti-Fe(1:1)/SFBC was generated from SFBC that was prepared by carbonization process at 500 °C for 2 h, and the resultant was impregnated by titanium tetraisopropoxide (500 μmol) and iron(III) nitrate (500 μmol) and calcined at 350 °C for 2 h. The codes of all catalysts are listed in Table 1.

Table 1. Types of samples and treatments

Samples	Type of treatment	Concentration of Ti (μmol)	Concentration of Fe (μmol)
FBC	-	-	-
SFBC	Sulfonation	-	-
Ti/ SFBC	Sulfonation	500	-
Fe/ SFBC	Sulfonation	-	500
Ti-Fe(1:1)/SFBC	Sulfonation	500	500
Ti-Fe(2:1)/SFBC	Sulfonation	1000	500
Ti-Fe(1:2)/SFBC	Sulfonation	500	1000

Catalysts characterization

The characterization of catalysts was performed by using FTIR, XRD, XRF, SEM, and BET surface area. FTIR spectrometer with a spectral resolution of 2 cm^{-1}, scans 10 s, temperature at 20 °C and wavenumber from 400 to 4000 cms^{-1}, was used to identify the functional groups in the catalyst. The crystallinity and phase content of the catalyst were analyzed using the XRD with the Cu Kα (λ = 1.5406 Å) radiation as the diffracted monochromatic beam at 40 kV and 40 mA. The pattern was scanned in the 2θ ranges between 7° and 60° at a step of 0.03° and step time of 1 s. The catalysts' chemical composition and physical properties were investigated using 1 kW wavelength dispersive XRF. The SEM with an accelerating voltage of 15 kV was used to determine the surface morphology and element containing the catalyst. The nitrogen adsorption-desorption isotherms were measured at a bath temperature of 77.3 K and an outgassed temperature of 300 °C using a Quantachrome NovaWIn instrument version 11.0.

Catalytic test

The performance of catalysts was evaluated by an oxidation of styrene with H_2O_2 as an oxidant. The procedure of reactions was conducted according to the previous research [25-27]. All reactions were performed by mixing styrene (5 mmol), H_2O_2 (30%, 5 mmol), acetonitrile (4.5 mL), and catalyst (0.1 g) with stirring for 24 h at room temperature. The products were then analyzed by GC and nitrogen as the carrier gas. The temperatures of the injector and detector were programmed at 250 and 260 °C, respectively. The column oven temperature was programmed to increase from 80 to 140 °C, at a rate of 10 °C/min.

■ RESULTS AND DISCUSSION

The results of WDXRF analysis revealed that calcium (Ca) and phosphorus (P) were the major elements in the FBC. After undergoing the processes of sulfonation, impregnation with titanium (Ti) and iron (Fe), and calcination, the samples were found to be dominated by calcium (Ca), sulfur (S), titanium (Ti), and iron (Fe). These aforementioned elements indicate the success of the sulfonation and metal impregnation processes. A comprehensive list of all the elements detected is provided in Table 2.

Fig. 1 displays the FTIR spectra of Ti-Fe (1:1)/SFBC, Ti-Fe (2:1)/SFBC, and Ti-Fe (1:2)/SFBC, which are compared to Fe_2O_3, TiO_2, and hydroxyapatite (HA). The spectra of all three Ti-Fe/SFBC samples (1:1, 2:1, and 1:2) are quite similar, indicating they share similar characteristics. Specifically, the absorption bands at 2500–3600 and 1626 cm^{-1} correspond to the stretching mode of the hydroxyl (O–H) group of organic compounds. The presence of HA in the sample is indicated by the carbonate ion (CO_3^{2-}) and phosphate ion (PO_4^{3-}) groups, which were detected through absorption bands at 2100–2450 cm^{-1} and wavenumbers ranging from 1150 to 460 cm^{-1}, respectively [28-33]. The P–O stretching asymmetric was identified by the absorption bands around 1150–1000 cm^{-1}. The bending vibration of PO_4^{3-} was observed through bands at 510–620 cm^{-1}, while the band at 874 cm^{-1} was assigned to the acidic phosphate group (HPO_4^{2-}) [34]. The presence of

Table 2. Elements analysis of Ti-Fe(1:1)/SFBC, Ti-Fe(1:2)/SFBC and Ti-Fe(2:1)/SFBC obtained using WDXRF

Elements	FBC	Ti-Fe (1:1)/SFBC	Ti-Fe (1:2)/SFBC	Ti-Fe (2:1)/SFBC
P	16.300	-	-	-
S	-	29.200	29.200	27.600
Ca	81.200	58.500	58.100	55.600
Ti	-	4.600	2.720	9.000
Fe	0.063	7.200	8.360	7.060
V	-	0.130	0.076	0.210
Cu	0.041	0.038	0.042	0.044
Sr	0.580	0.350	0.350	0.310

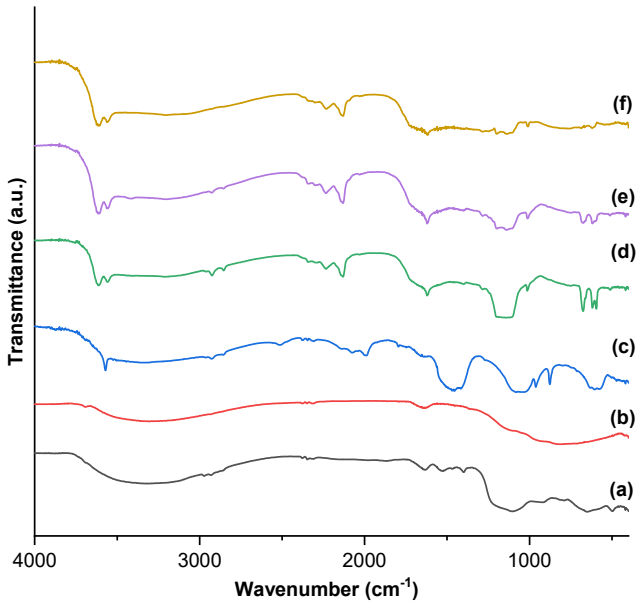

Fig 1. FTIR spectra of (a) Fe_2O_3, (b) TiO_2, (c) HA, (d) Ti-Fe(1:1)/SFBC, (e) Ti-Fe(2:1)/SFBC, and (f) Ti-Fe(1:2)/SFBC

iron was identified through absorptions around 540 and 442 cm^{-1}, which have been associated with Fe–O vibrations of Fe_2O_3 [31]. Framework titanium was characterized by an adsorption band in the 900–975 cm^{-1} range, which was attributed to symmetric O–Ti–O stretching that caused the vibration of the Ti–O bond. In Fig. 1(d) and (f), the absorption around 900–975 cm^{-1} is not detected due to the small amount of titanium, but it appears after the titanium was doubled, as seen in Fig. 1(e).

The XRD pattern in Fig. 2 was used to determine the crystallinity of Ti-Fe(1:1)/SFBC, Ti-Fe(2:1)/SFBC, and Ti-Fe(1:2)/SFBC, as well as control samples of Fe_2O_3, TiO_2, and HA. The HA crystallinity (JCPDS-PDF 74-0565) was identified in Fig. 2(a) by the diffraction peaks at 2θ = 25.8, 32.0, 39.7, 46.8, 49.4, and 53.0. The Fe_2O_3 crystallinity was determined in Fig. 2(b) by the diffraction peaks at 2θ = 25.2, 36.9, 37.7, 38.5, 47.9, 53.8, and 54.9. The crystallinity of Ti-Fe(1:1)/SFBC, Ti-Fe(2:1)/SFBC, and Ti-Fe(1:2)/SFBC was found to be almost the same at 52.2, 46.1, and 50.1%, respectively. In all three Ti-Fe/SFBC samples, the presence of titanium, iron, and HA crystals was detected through diffraction peaks at 2θ = 25.2 and 38.5 for titanium; 2θ = 40.8, 43.5, and 49.4 for iron; and 2θ = 22.8, 31.6, 32.8, and 57.1 for HA.

Fig. 3 displays the SEM images of FBC, Ti-Fe(1:1)/SFBC, Ti-Fe(1:2)/SFBC, and Ti-Fe(2:1)/SFBC. All samples exhibited rough and irregular surface morphology [35]. The surface area and pore structure of all samples were determined through Nitrogen adsorption-desorption isotherm analysis. Fig. 4 shows the isotherms for Ti-Fe(1:1)/SFBC, Ti-Fe(1:2)/SFBC, and

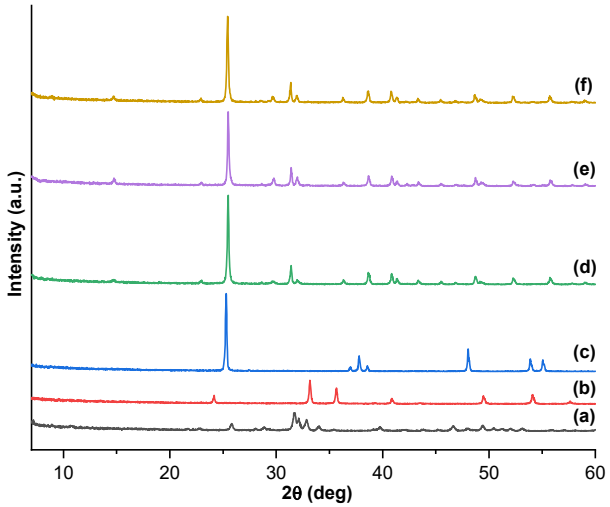

Fig 2. XRD pattern of (a) HA, (b) Fe_2O_3, (c) TiO_2, (d) Ti-Fe(1:1)/FBC, (d) Ti-Fe(1:1)/SFBC, (e) Ti-Fe(2:1)/SFBC, and (f) Ti-Fe(1:2)/SFBC

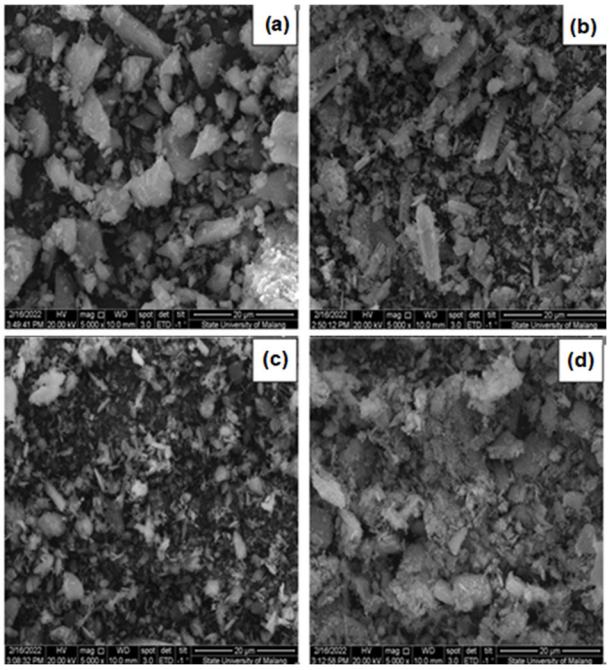

Fig 3. SEM Image of (a) CFB, (b) Ti-Fe(1:1)/FBC, (c) Ti-Fe(1:2)/FBC, and (d) Ti-Fe(2:1)/FBC

Ti-Fe(2:1)/SFBC, which were all classified as Type IV according to IUPAC, typical for mesoporous materials. The isotherms exhibited narrow hysteresis loops in the relative pressure range of ~0.6–1.0 (Ti-Fe(1:1)/SFBC), ~0.5–1.0 (Ti-Fe(1:2)/SFBC), and ~0.55–1.0 (Ti-Fe(2:1)/SFBC).

Table 3 presents the surface area, pore volume, and mean pore size for all samples. The presence of uniform mesopores was indicated by mean pore sizes greater than 2 nm. Metal impregnation (Ti and Fe) was found to increase the surface area, with Ti impregnation resulting in a higher increase than Fe impregnation.

Catalytic Performance

The yields of styrene oxidation products catalyzed by SFBC-loaded titanium-iron oxides are presented in Table 4. The primary products obtained using H_2O_2 as an oxidant were benzaldehyde, phenylacetaldehyde, and styrene oxide, with benzaldehyde being the dominant product. The mechanism starts from the adsorption of H_2O_2 on bimetallic oxides/SFBC, followed by the formation of hydroperoxyl species, then transfer of oxygen from bimetallic oxides to styrene, finally cleavage of the metalloepoxy intermediate, and also cleavage of the C=C bond (Fig. 5).

To compare, FBC, SFBC, Ti/SFBC, and Fe/SFBC were also used as catalysts for styrene oxidation. The performance of each catalyst was evaluated based on styrene conversion and benzaldehyde selectivity. FBC exhibited a styrene conversion of 0.7% and benzaldehyde selectivity of 35% at room temperature for 24 h. SFBC, however, showed increased performance with a styrene conversion of 2.6% and benzaldehyde selectivity of 93%. The presence of $–SO_3H$ groups resulting from the sulfonation process of FBC influenced the catalytic performance of SFBC.

To evaluate the influence of titanium and iron, Ti/SFBC and Fe/SFBC were compared with the Ti-Fe/SFBC catalyst. Ti/SFBC showed higher catalytic activity than Fe/SFBC, with a styrene conversion of 23% and benzaldehyde selectivity of 90, 12, and 73%, respectively. The styrene conversion and benzaldehyde

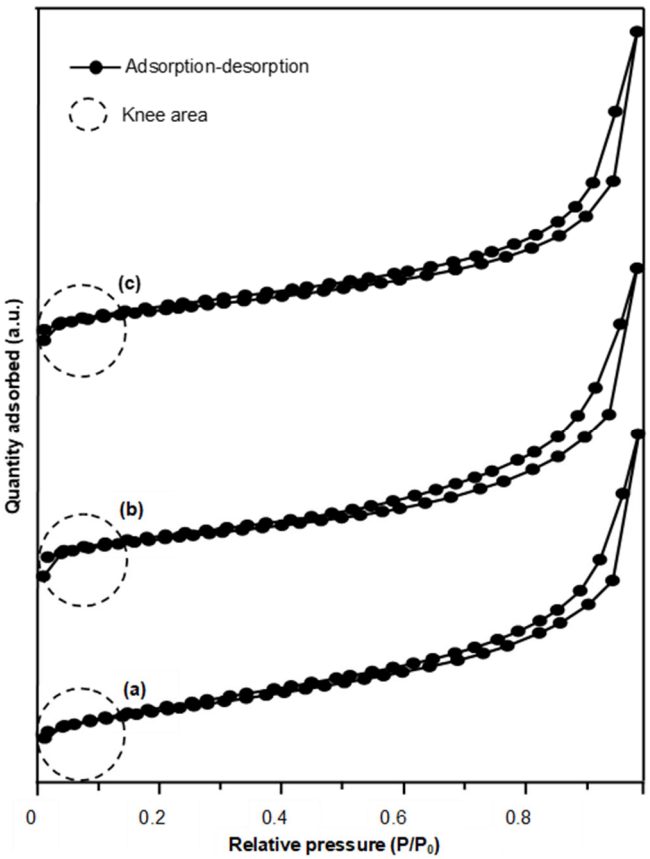

Fig 4. The physisorption isotherms of (a) Ti-Fe(1:1)/FBC, (b) Ti-Fe(1:2)/FBC, and (c) Ti-Fe(2:1)/FBC

Table 3. Physical properties of the catalysts

Samples	BET surface area (m^2/g)	Pore volume (cm^3/g)	Mean pore size (nm)
SCFB	6.8	0.0147	4.3
Ti/SCFB	13.9	0.0350	5.0
Fe/SCFB	7.6	0.0386	10.2
Ti-Fe(1:1)/SCFB	35.1	0.1172	6.7
Ti-Fe(2:1)/SCFB	34.8	0.1122	6.4
Ti-Fe(1:2)/SCFB	16.9	0.0616	7.3

Table 4. Catalytic performance of the catalysts in the oxidation of styrene

Catalyst	Conversion (%)[a]	Selectivity (%)			
		BzA[b]	PhA[c]	SO[d]	Other
FBC	0.7	34.6	13.1	17.1	35.2
SFBC	2.6	93.4	0.0	3.5	3.1
Ti/SFBC	23.0	90.0	3.0	3.0	4.0
Fe/SFBC	11.6	73.0	0.4	7.0	19.6
Ti-Fe(1:1)/SFBC	41.2	90.8	0.7	0.5	8.0
Ti-Fe(2:1)/SFBC	44.2	88.8	0.5	4.1	6.6
Ti-Fe(1:2)/SFBC	29.3	92.9	1.2	1.5	4.4

[a] Reaction conditions: The reactions were carried out at room temperature for 24 h with styrene (5 mmol), 30% H_2O_2 (5 mmol), and catalyst (100 mg). BzA[b] = benzaldehyde, PhA[c] = phenylacetaldehyde, and SO[d] = styrene oxide

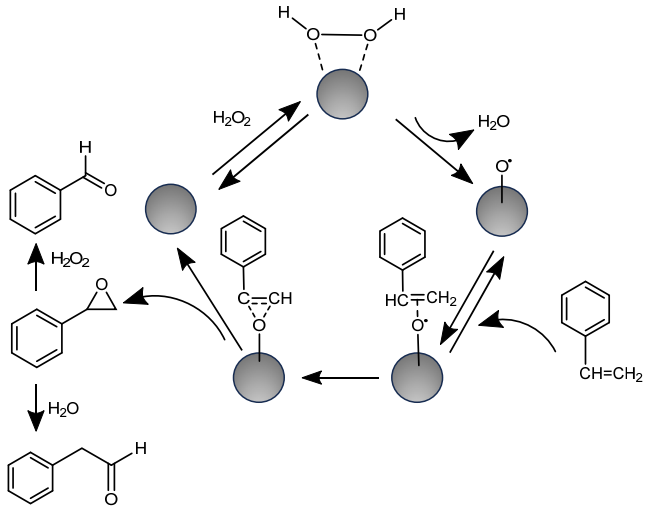

Fig 5. The mechanistic pathway of styrene oxidation using bimetallic oxides loaded sulfonated carbon-derived fishbone catalyst

selectivity were further increased to 41 and 88% for Ti-Fe(1:1)/SFBC, 44 and 88% for Ti-Fe(2:1)/SFBC, and 29 and 93% for Ti-Fe(1:2)/SFBC, respectively. The higher catalytic performance of Ti-Fe(1:1)/SFBC can be attributed to its higher total surface area compared to Ti/SFBC and Fe/SFBC. Doubling the number of titanium active sites did not affect the styrene oxidation conversion because it was not accompanied by an increase in the catalyst's surface area. However, doubling the number of iron active sites led to a decrease in styrene oxidation conversion due to a decrease in the surface area of the catalyst. These results are consistent with previous studies, which found that adding Ti and Fe active sites does not necessarily increase styrene conversion, and Fe impregnation leads to lower styrene conversion compared to Ti impregnation [13]. The above results reveal that the presence of both titanium and iron oxides on the surface of SFBC and the catalyst's surface area creates a synergistic effect, which are the primary factors affecting its catalytic activity in styrene oxidation using H_2O_2 as an oxidant. This synergistic effect can be attributed to several scientific reasons [36-39].

Firstly, incorporating titanium and iron oxides provides multiple active sites on the catalyst surface. These active sites are crucial for enhancing the catalytic activity because they facilitate the adsorption and activation of the reactants, as well as the desorption of the products. Consequently, the presence of both metals can enhance the catalytic performance by promoting the interaction between the reactants and the catalyst surface. Secondly, the combination of titanium and iron oxides may result in the formation of mixed metal oxide phases. These mixed phases can exhibit unique electronic and structural properties enhancing the catalytic activity. For instance, the formation of mixed phases can lead to improved electron transfer between the metals, which can, in turn, facilitate the activation of the reactants and the subsequent oxidation reactions.

Moreover, the presence of both titanium and iron oxides can also lead to the formation of a more porous catalyst structure, which can increase the surface area available for catalytic reactions. As demonstrated in Table 2, the bimetallic catalyst, Ti-Fe (1:1)/SFBC, has a

higher total surface area compared to the monometallic catalysts, Ti/SFBC and Fe/SFBC. A higher surface area is crucial for catalytic activity, as it increases the number of active sites available for the reactants to interact with, thus promoting the oxidation reaction.

However, it is essential to note that simply increasing the number of active sites for one of the metals does not necessarily lead to a higher conversion of styrene. For instance, when the number of titanium active sites was doubled (Ti-Fe(2:1)/SFBC), it did not result in an increase in styrene oxidation conversion due to the absence of a corresponding increase in the catalyst's surface area. Furthermore, when the number of iron active sites was doubled (Ti-Fe(1:2)/SFBC), the styrene oxidation conversion decreased, as the addition of iron active sites led to a reduction in the catalyst's surface area.

The synergistic effect observed in the Ti-Fe/SFBC catalyst for styrene oxidation can be attributed to the presence of both titanium and iron oxides, which provide multiple active sites, promote the formation of mixed metal oxide phases, and contribute to a higher surface area. However, it is crucial to maintain a proper balance between the active sites and the catalyst's surface area to optimize the catalytic performance.

The study has several limitations that should be considered. First, it is focused solely on the Ti-Fe/SFBC catalyst for styrene oxidation, which means that the findings may not apply to other types of catalysts or reaction systems. Second, the investigation of the relationship between catalyst structure and catalytic properties is limited by the techniques and methods used in this study, which may not capture all aspects of the catalyst's behavior. Lastly, the study does not address the long-term stability and reusability of the Ti-Fe/SFBC catalyst, which are important factors for practical applications.

To gain a deeper understanding of the synergistic effect and the relationship between catalyst structure and catalytic properties, further studies should explore several aspects. Investigate the Ti-Fe/SFBC catalyst's performance in other oxidation reactions to assess the generality of the observed synergistic effect. Employ advanced characterization techniques to gain a more detailed understanding of the catalyst's structure, including the nature of the active sites and the interaction between titanium and iron oxides. Examine the effect of varying the ratio of titanium and iron oxides in the catalyst to identify the optimal balance between active sites and surface area for enhanced catalytic performance. Lastly, evaluate the long-term stability and reusability of the Ti-Fe/SFBC catalyst under various reaction conditions to determine its practical applicability. By addressing these aspects, future studies can contribute to developing more efficient and versatile catalysts for styrene oxidation and other related reactions.

To check the reusability and stability of the Ti-Fe(1:1)/SFBC, Ti-Fe(2:1)/SFBC, and Ti-Fe(1:2)/SFBC, all catalysts were recovered and recycled for further reaction.

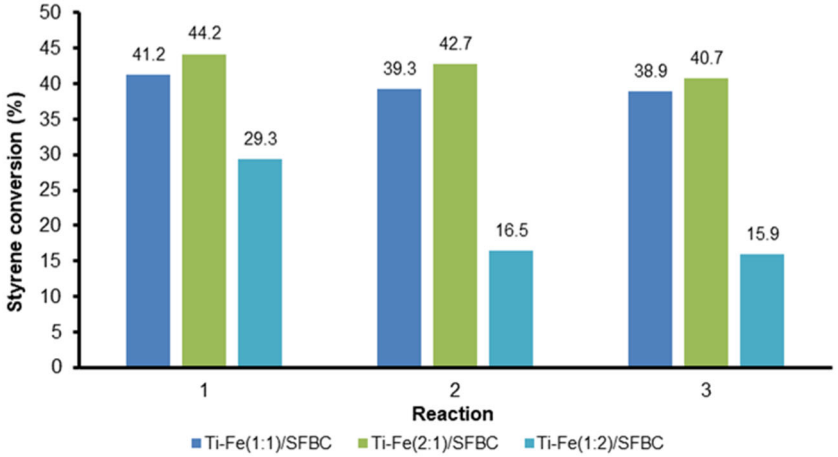

Fig 6. The reuse of catalysts in the oxidation of styrene (5 mmol), 30% H_2O_2 (5 mmol) and catalyst (100 mg) at room temperature for 24 h

After each use, both catalysts were recycled by washing with ethanol and centrifugation thrice and drying at 110 °C in a vacuum oven overnight. The conversion of styrene oxidation was used to compare all catalysts. As shown in Fig. 6, Ti-Fe(1:1)/SFBC and Ti-Fe(2:1)/SFBC catalysts were higher and more stable after three reaction cycles than Ti-Fe(1:2)/SFBC catalyst. The decrease in the styrene conversion from the first reaction cycle to the second and third reaction cycles were 44.2, 42.7, and 40.7% for Ti-Fe(2:1)/SFBC; 41.2, 39.3, and 38.9% for Ti-Fe(1:1)/SFBC. Different from the Ti-Fe(1:2)/SFBC catalyst, the decrease in the yield of styrene conversion was very drastic at 29.3, 16.5, and 15.9%. Based on catalytic performance for styrene oxidation with H_2O_2 as oxidant, after three cycles of reaction and wash, we predicted that around 94% of the Ti-Fe(1:1)/SFBC, 92% of Ti-Fe(2:1)/SFBC, and 54% catalytic sites of fresh catalysts should remain on the catalyst under the reaction conditions used in this study. The explanation might be used as the physical loss of some catalyst powder during the recycling step. During the washing step, titanium and iron active sites directly interact with ethanol as the solvent; hence, the leaching cannot be avoided.

■ CONCLUSION

The utilization of bimetallic titanium-iron oxide loaded SFBC as a catalyst has been investigated in the oxidation of styrene using aqueous H_2O_2. The study found that the catalytic performance of SFBC was superior to that of FBC, and Ti/SFBC was greater than Fe/SFBC. A synergistic effect was observed due to the coexistence of titanium (Ti) and iron (Fe) oxides, which enhanced the catalytic performance. The presence of titanium and iron oxides influenced the surface area and the catalytic activity of the catalysts in the oxidation of styrene, employing aqueous H_2O_2 as an oxidant. Upon examining reusability and stability, it was concluded that a specific ratio of Ti-Fe/SFBC demonstrated better stability compared to other Ti-Fe/SFBC ratios.

■ ACKNOWLEDGMENTS

The authors gratefully acknowledge the research grant from the Ministry of Education, Culture, Research and Technology of the Republic of Indonesia by contract number: 297/UN17.L1/HK/2022.

■ AUTHOR CONTRIBUTIONS

Mukhamad Nurhadi: conceptualization, methodology, supervision, investigation, resources, data curation, writing, review, and editing; Ratna Kusumawardani: conceptualization, methodology, formal analysis, data curation, writing draft preparation, and project administration; Teguh Wirawan: conceptualization, methodology, investigation, resources, data curation, and writing draft preparation; Sin Yuan Lai: proofreading, writing, review, and editing; Hadi Nur: proofreading, writing, review, and editing. All authors have read and agreed to the published version of the manuscript.

■ REFERENCES

[1] Ito, S., Kon, Y., Nakashima, T., Hong, D., Konno, H., Ino, D., and Sato, K., 2019, Titania-catalyzed H_2O_2 thermal oxidation of styrenes to aldehydes, *Molecules*, 24 (14), 2520.

[2] Batra, M.S., Dwivedi, R., and Prasad, R., 2019, Recent developments in heterogeneous catalyzed epoxidation of styrene to styrene oxide, *ChemistrySelect*, 4 (40), 11636–11673.

[3] Andrade, M.A., and Martins, L.M.D.R.S., 2021, Selective styrene oxidation to benzaldehyde over recently developed heterogeneous catalysts, *Molecules*, 26 (6), 1680.

[4] Aberkouks, A., Mekkaoui, A.A., Boualy, B., El Houssame, S., Ait Ali, M., and El Firdoussi, L., 2018, Selective oxidation of styrene to benzaldehyde by Co-Ag codoped ZnO catalyst and H_2O_2 as oxidant, *Adv. Mater. Sci. Eng.*, 2018, 2716435.

[5] Xie, L., Wang, H., Lu, B., Zhao, J., and Cai, Q., 2018, Highly selective oxidation of styrene to benzaldehyde over Fe_3O_4 using H_2O_2 aqueous solution as oxidant, *React. Kinet., Mech. Catal.*, 125 (2), 743–756.

[6] Sakthivel, B., Josephine, D.S.R., Sethuraman, K., and Dhakshinamoorthy, A., 2018, Oxidation of styrene using TiO_2-graphene oxide composite as

solid heterogeneous catalyst with hydroperoxide as oxidant, *Catal. Commun.*, 108, 41–45.

[7] Hulea, V., and Dumitriu, E., 2004, tyrene oxidation with H_2O_2 over Ti-containing molecular sieves with MFI, BEA and MCM-41 topologies, *Appl. Catal., A*, 277 (1-2), 99–106.

[8] Jafarpour, M., Ghahramaninezhad, M., and Rezaeifard, A., 2014, Catalytic activity and selectivity of reusable α-MoO_3 nanobelts toward oxidation of olefins and sulfides using economical peroxides, *RSC Adv.*, 4 (4), 1601–1608.

[9] Wang, H., Qian, W., Chen, J., Wu, Y., Xu, X., Wang, J., and Kong, Y., 2014, Spherical V-MCM-48: The synthesis, characterization and catalytic performance in styrene oxidation, *RSC Adv.*, 4 (92), 50832–50839.

[10] Cancino, P., Paredes-García, V., Aguirre, P., and Spodine, E., 2014, A reusable Cu^{II} based metal–organic framework as a catalyst for the oxidation of olefins, *Catal. Sci. Technol.*, 4 (8), 2599–2607.

[11] Zhang, Y., Wei, N., Xing, Z., and Han, Z.B., 2020, Functional hexanuclear Y(III) cluster-based MOFs supported Pd(II) single site catalysts for aerobic selective oxidation of styrene, *Appl. Catal., A*, 602, 117668.

[12] Nurhadi, M., Kusumawardani, R., Wirawan, T., Sumari, S., Lai, S.Y., and Nur, H., 2021, Catalytic performance of TiO_2–carbon mesoporous-derived from fish bones in styrene oxidation with aqueous hydrogen peroxide as an oxidant, *Bull. Chem. React. Eng. Catal.*, 16 (1), 88–96.

[13] Tanglumlert, W., Imae, T., White, T.J., and Wongkasemjit, S., 2009, Styrene oxidation with H_2O_2 over Fe- and Ti-SBA-1 mesoporous silica, *Catal. Commun.*, 10 (7), 1070–1073.

[14] Kusumawardani, R., Nurhadi, M., Wirawan, T., Prasetyo, A., Agusti, N.N., Lai, S.Y., and Nur, H., 2022, Kinetic study of styrene oxidation over titania catalyst supported on sulfonated fish bone-derived carbon, *Bull. Chem. React. Eng. Catal.*, 17 (1), 194–204.

[15] Ha, Y., Mu, M., Liu, Q., Ji, N., Song, C., and Ma, D., 2017, Mn-MIL-100 heterogeneous catalyst for the selective oxidative cleavage of alkenes to aldehydes, *Catal. Commun.*, 103, 51–55.

[16] Ghosh, R., Son, Y.C., Makwana, V.D., and Suib, S.L., 2004, Liquid-phase epoxidation of olefins by manganese oxide octahedral molecular sieves, *J. Catal.*, 224 (2), 288–296.

[17] Zou, H., Xiao, G., Chen, K., and Peng, X., 2018, Noble metal free V_2O_5/g-C_3N_4 composite for selective oxidation of olefins using hydrogen peroxide as oxidant, *Dalton Trans.*, 47 (38), 13565–13572.

[18] Saux, C., and Pierella, L.B., 2011, Studies on styrene selective oxidation to benzaldehyde catalyzed by Cr-ZSM-5: Reaction parameters effects and kinetics, *Appl. Catal., A*, 400 (1-2), 117–121.

[19] Fiorenza, R., 2020, Bimetallic catalysts for volatile organic compound oxidation, *Catalysts*, 10 (6), 661.

[20] Vetrivel, S., and Pandurangan, A., 2005, Supported metal oxide catalysts: Their activity to vapor phase oxidation of ethylbenzene, *Ind. Eng. Chem. Res.*, 44 (4), 692–701.

[21] Das, S., Gupta, A., Singh, D., and Mahajani, S., 2019, La/Zn bimetallic oxide catalyst for epoxidation of styrene by cumene hydroperoxide: Kinetics and reaction engineering aspects, *Ind. Eng. Chem. Res.*, 58, 7448–7460.

[22] Zhang, Y., Wang, H., Li, S., Lu, B., Zhao, J., and Cai, Q., 2021, Catalytic oxidation of styrene and its reaction mechanism consideration over bimetal modified phosphotungstates, *Mol. Catal.*, 515, 111940.

[23] Huang, K., Yu, S., Li, X., and Cai, Z., 2020, One-pot synthesis of bimetal MOFs as highly efficient catalysts for selective oxidation of styrene, *J. Chem. Sci.*, 132 (1), 139.

[24] Zou, H., Hu, C., Chen, K., Xiao, G., and Peng, X., 2018, Cobalt vanadium oxide supported on reduced graphene oxide for the oxidation of styrene derivatives to aldehydes with hydrogen peroxide as oxidant, *Synlett*, 29 (16), 2181–2184.

[25] Nurhadi, M., 2017, Modification of coal char-loaded TiO_2 by sulfonation and alkylsilylation to enhance catalytic activity in styrene oxidation with hydrogen peroxide as oxidant, *Bull. Chem. React. Eng. Catal.*, 12 (1), 55–61.

[26] Nurhadi, M., Efendi, J., Lee, S.L., Indra Mahlia, T.M.,

Chandren, S., Ho, C.S., and Nur, H., 2015, Utilization of low rank coal as oxidation catalyst by controllable removal of its carbonaceous component, *J. Taiwan Inst. Chem. Eng.*, 46, 183–190.

[27] Nurhadi, M., Chandren, S., Yuan, L.S., Ho, C.S., Indra Mahlia, T.M., and Nur, H., 2017, Titania-loaded coal char as catalyst in oxidation of styrene with aqueous hydrogen peroxide, *Int. J. Chem. React. Eng.*, 15 (1), 20160088.

[28] Chakraborty, R., and Chowdhury, D.R., 2013, Fish bone derived natural hydroxyapatite-supported copper acid catalyst: Taguchi optimization of semibatch oleic acid esterification, *Chem. Eng. J.*, 215-216, 491–499.

[29] Patel, S., Han, J., Qiu, W., and Gao, W., 2015, Synthesis and characterisation of mesoporous bone char obtained by pyrolysis of animal bones, for environmental application, *J. Environ. Chem. Eng.*, 3 (4, Part A), 2368–2377.

[30] Yin, T., Park, J.W., and Xiong, S., 2015, Physicochemical properties of nano fish bone prepared by wet media milling, *LWT - Food Sci. Technol.*, 64 (1), 367–373.

[31] Zayed, E.M., Sokker, H.H., Albishri, H.M., and Farag, A.M., 2013, Potential use of novel modified fishbone for anchoring hazardous metal ions from their solutions, *Ecol. Eng.*, 61, 390–393.

[32] Lestari, S., Nurhadi, M., Kusumawardani, R., Saputro, E., Pujisupiati, R., Muskita, N.S., Fortuna, N., Purwandari, A.S., Aryani, F., Lai, S.Y., and Nur, H., 2022, Comparative adsorption performance of carbon-containing hydroxyapatite derived tenggiri (*Scomberomorini*) and belida (*Chitala*) fish bone for methylene blue, *Bull. Chem. React. Eng. Catal.*, 17 (3), 565–576.

[33] Nurhadi, M., Kusumawardani, R., Nurhadi, M., Wirhanuddin, W., Gunawan, R., and Nur, H., 2019, Carbon-containing hydroxyapatite obtained from fish bone as low-cost mesoporous material for methylene blue adsorption, *Bull. Chem. React. Eng. Catal.*, 14 (3), 660–671.

[34] Jaber, H.L., Hammood, A.S., and Parvin, N., 2018, Synthesis and characterization of hydroxyapatite powder from natural *Camelus* bone, *J. Aust. Ceram. Soc.*, 54 (1), 1–10.

[35] Abdullah, N.H., Mohamed Noor, A., Mat Rasat, M.S., Mamat, S., Mohamed, M., Mohd Shohaimi, N.A., Ab Halim, A.Z., Mohd Shukri, N., Azhar Abdul Razab, M.K., and Mohd Amin, M.F., 2020, Preparation and characterization of calcium hydroxyphosphate (hydroxyapatite) from tilapia fish bones and scales via calcination method, *Mater. Sci. Forum*, 1010, 596–601.

[36] Goulas, K.A., Sreekumar, S., Song, Y., Kharidehal, P., Gunbas, G., Dietrich, P.J., Johnson, G.R., Wang, Y.C., Grippo, A.M., Grabow, L.C., Gokhale, A.A., and Toste, F.D., 2016, Synergistic effects in bimetallic palladium–copper catalysts improve selectivity in oxygenate coupling reactions, *J. Am. Chem. Soc.*, 138 (21), 6805–6812.

[37] He, L., Gong, X., Ye, L., Duan, X., and Yuan, Y., 2016, Synergistic effects of bimetallic Cu-Fe/SiO_2 nanocatalysts in selective hydrogenation of diethyl malonate to 1,3-propanediol, *J. Energy Chem.*, 25 (6), 1038–1044.

[38] Stucchi, M., Capelli, S., Cardaci, S., Cattaneo, S., Jouve, A., Beck, A., Sáfrán, G., Evangelisti, C., Villa, A., and Prati, L., 2020, Synergistic effect in Au-Cu bimetallic catalysts for the valorization of lignin-derived compounds, *Catalysts*, 10 (3), 332.

[39] Ehsan, M.A., Hakeem, A.S., and Rehman, A., 2020, Synergistic effects in bimetallic Pd–CoO electrocatalytic thin films for oxygen evolution reaction, *Sci. Rep.*, 10 (1), 14469.